

a306872  
CPUB

NICKEL-MOLYBDENUM/ALUMINA CATALYSTS:  
EFFECTS OF DOPING WITH FLUORIDE AND LITHIUM  
AND CHANGES IN PARTICULATE SIZE WHEN APPLIED TO  
BITUMEN HYDROPROCESSING

J.F. Kriz, J. Monnier and M. Ternan  
MAY 1990

ERL 90-0500 (OP,J)  
ENERGY RESEARCH LABORATORIES  
DIVISION REPORT ERL 90- (OP,J)  
90-0500  
CPUB

ERL 90-0500 (OP,J)



a 306872  
CPUB

NICKEL-MOLYBDENUM/ALUMINA CATALYSTS:  
EFFECTS OF DOPING WITH FLUORIDE AND LITHIUM, AND CHANGES IN  
PARTICULATE SIZE WHEN APPLIED TO BITUMEN HYDROPROCESSING

J.F. Kriz, J. Monnier and M. Ternan

Energy Research Laboratories, CANMET, EMR Canada, 555 Booth St., Ottawa, Ont. K1A 0G1

INTRODUCTION

This study was undertaken as part of a research program addressing the conversion of Canadian bitumens, and heavy and residual oils to high quality fuels. Previously, catalysts modified by additions of alkali (1) and fluoride (2) compounds were tested in this laboratory for hydroprocessing of such feeds. Performance improvements noted after fluoride doping were further investigated elsewhere using model reactions for cracking (3, 4), hydrogenolysis and hydrodesulphurization (5, 6). Among the many possible effects that the catalyst modifications may have caused were the changes in metal dispersion and in diffusional limitations. These appeared to be important for reactions involving large molecules and were considered worth further investigation. Catalysts in this work were modified by additions of both fluoride and lithium. Diffusional effects were examined by using two different particulate sizes of the same catalyst formulations.

EXPERIMENTAL

The catalysts were evaluated in a continuous flow hydrocracking reactor with Athabasca bitumen (Table 1) at 13.9 MPa pressure,  $1 \text{ h}^{-1}$  liquid space velocity,  $36 \text{ mL s}^{-1}$  hydrogen flow at STP (5000 scf/bbl) and  $420^\circ\text{C}$  reactor temperature. Hydrogen and bitumen were mixed together and flowed up through a fixed bed of catalyst particles (extrudates or grains). The catalyst bed had a volume 155 mL and a length to diameter ratio 12.

Catalyst Preparations

Table 2 summarizes the catalyst specifications and identifications. The base catalyst, further referred to as B, was prepared by spray-mix-mulling of acidified alpha-alumina monohydrate (Catapal SB obtained from Continental Oil Company, Peterboro, N.J.). Aqueous solutions of nickel nitrate and ammonium paramolybdate were added in this sequence. Appropriate concentrations and amounts were added, and the resulting paste was extruded into 3.2 mm (1/8") extrudates which were dried for 5 h at  $120^\circ\text{C}$  and calcined for 5 h at  $500^\circ\text{C}$ . A thin layer of part of the paste was dried and calcined on tray without extruding. The resulting catalyst contained about 15 wt %  $\text{MoO}_3$  and 4 wt % NiO having atomic ratios Ni:Mo:Al = 1:2:30.

The fluoride-impregnated catalyst further referred to as F/B was prepared from B by adding an ammoniacal solution of ammonium bifluoride  $\text{NH}_4\text{FHF}$  and recalcining. The catalyst identified as F/B\* was prepared from unextruded B and sieved to U.S. MESH -8+30 (0.6-2.38 mm diameter grains). The resulting atomic ratios were Mo:F = 2:3.

The lithium-impregnated catalyst further referred to as LL/B was prepared from B by adding an aqueous solution of lithium nitrate  $\text{LiNO}_3$  and recalcining. The resulting atomic ratios were Mo:Li = 2:3.



CPUB

The lithium-impregnated fluorided catalysts further referred to as LF/B and LF/B\* were prepared from F/B and F/B\*, respectively, by adding the solution of lithium nitrate and recalcining. The resulting atomic ratios were Li:F = 1:3.

The lithium-impregnated fluorided catalyst further referred to as LLF/B was prepared from F/B in the same manner as LF/B. The resulting atomic ratios were Mo:Li:F = 2:3:3.

The lithium-alumina dry-mix support was prepared by mixing the alumina monohydrate with lithium carbonate  $\text{Li}_2\text{CO}_3$  powder. The resulting mixture was used as in the case of B preparation to prepare the catalyst further referred to as BL having atomic ratios Ni:Mo:Li:Al = 1:2:3:30.

The lithium-mixed fluoride-impregnated catalyst further referred to as F/BL was prepared from BL by adding the solution of ammonium bifluoride and recalcining. The resulting atomic ratios were Mo:Li:F = 2:3:3.

The lithium-mixed fluoride-impregnated catalyst further referred to as FF/BL was prepared from BL in the same manner as F/BL. The resulting atomic ratios were Mo:Li:F = 2:3:6.

## RESULTS AND DISCUSSION

### Effects on Performance Criteria and Ranking

The results of liquid product analyses are shown in Table 3. These include relative densities and contents of carbon, hydrogen, sulphur, nitrogen and 525°C+ pitch. Also shown are boiling temperatures at two different distilled-off percentages.

Based on the T.O.S. (time on stream) averages of the data in Table 3, the catalysts as identified in the experimental section can be ranked depending on the pertinent performance criteria, noted on the left hand side:

Lower relative density:

F/B > LF/B > F/B\* > LF/B\* > LLF/B > FF/BL > B > F/BL > LL/B > BL

Lower b.p. at 10 % off:

LL/B > F/BL > B > F/B > FF/BL > LF/B > BL > LLF/B > F/B\* > LF/B\*

Lower b.p. at 50 % off:

F/B > LF/B > B > LL/B > BL > LLF/B > F/B\* > LF/B\* > FF/BL > F/BL

Higher pitch conversion:

B > F/B\* > LF/B > LL/B > F/B > LF/B\* > FF/BL > LLF/B > F/BL > BL

Higher H/C ratio:

F/B\* > LF/B\* > LF/B > LLF/B > F/B > F/BL > FF/BL > B > BL > LL/B

Higher sulphur removal:

F/B\* > LF/B\* > LLF/B > LF/B > FF/BL > B > F/B > F/BL > BL > LL/B

Higher nitrogen removal:

F/B\* > F/B > LF/B\* > LLF/B > LF/B > FF/BL > B > F/BL > LL/B > BL

The accuracy of catalyst ranking is limited in two aspects. One relates to an analytical error while the other to the processing sensitivity. Two separate samples of the liquid produced using the catalyst F/B\* were analyzed to establish the uncertainty governed by the analytical error. T.O.S. averages for density, sulphur, nitrogen and pitch indicated good reproducibility, while individual T.O.S. data showed some inconsistencies in sulphur and particularly nitrogen and H/C ratio. These inconsistencies allude to an uncertainty within the ranking order for HDN and hydrogenation selectivity of 3 to 4 places out of the 10 catalysts evaluated. Such an uncertainty indicates that the analytical error is approaching in magnitude the differences brought about by using the variety of catalysts and/or by the different T.O.S. However, even those liquid product properties that can be analyzed accurately, may prove to be insensitive to changing catalysts and/or T.O.S. For example, whereas the liquid product relative density in this study reflected the changes in catalysts and T.O.S. quite sensitively, the liquid yield seemed to vary almost randomly around 90 wt % irrespective of the T.O.S. or catalyst used. One of the problems with maintaining the processing precision stems from the experimental difficulty of retrieving the whole product pitch fraction, which accumulated in the receiver vessel during the run. The pitch tends to precipitate out of the product mixture and adhere to the vessel walls.

### Ranking in Activity and Selectivity

The base Ni-Mo/Alumina catalyst B showed good overall performance, ranking first in pitch conversion, better than average in yielding light and low-boiling distillates, average in density, HDS and HDN, and perhaps less than average in hydrogenation. Its ranking in general indicates good molecular weight reduction capability and selective cracking of large molecules. Actually, this type of catalyst is preferred in refining situations where hydrogenation and HDN are the primary goals. Its ranking thus suggests that the modifications studied can lead to improvements.

Fluoride impregnation (catalyst F/B) generally boosted the hydroprocessing capability of the base catalyst. F/B ranked first in lowering liquid product density, producing light distillates and HDN, and was above average in hydrogenation. It averaged in the rest of the performance indicators including the tendency to produce a low-boiling distillate, pitch conversion and HDS. The HDS performance is quite consistent with the findings of Lewis *et al* (6) that the synergism between fluoride and the metal components does not extend to the thiophene HDS. The changes in performance allude to an improved hydrogenation capability and associated cleavage of the C-N bond. Since the nitrogenates prevail among the larger and denser molecules, their hydrogenolysis reduces the overall product density and enhances the light distillate yield. On the other hand, the C-C cracking function seems to have receded since the pitch conversion and yield of low-boiling distillates became less extensive than in the case of the previous catalyst.

Lithium impregnation (catalyst LL/B) generally degraded the hydroprocessing capability of the base catalyst. Although LL/B ranked first in low-boiling distillate yield, it ranked lower than B in all other aspects, being notably behind in hydrogenation and heteroatom removal. The low-boiling yield can be interpreted in terms of an increased C-C cracking tendency. However, an opposite trend is indicated by ranking in pitch conversion where B is ahead of LL/B. Thus this cracking activity seems to be limited to small hydrocarbon molecules.

The influence of lithium impregnation of the fluorided base (catalysts LF/B and LLF/B) appears to be somewhat ambiguous. While it inhibits the lowering of product density, the yield of both light and low-boiling distillates, and HDN, it tends to promote HDS and hydrogenation, with mixed effects on pitch conversion. Furthermore, the effect of lithium loading suggests that the performance is impeded by higher loading (LLF/B vs. LF/B) in all aspects but HDS and HDN. Although any interpretation here would be doubtful because of the processing and analytical uncertainties involved, the overall effect of lithium impregnation can be seen as redundant, at best, from a pragmatic point of view.



The use of alumina and lithium carbonate mixtures as supports brought about undesirable changes in performance. In this case the effects observed are more consistent than in the case of lithium impregnation, and less dependent on whether fluoriding was done (catalysts F/BL and FF/BL) or not (catalyst BL). B outperformed BL in all aspects, while F/B outperformed F/BL in all but the yield of low-boiling distillate, and FF/BL in all but HDS. The yield of light distillate seems to be particularly inhibited. A comparison of F/BL with FF/BL alone (which differ in fluoride loading) shows FF/BL to be marginally ahead in all aspects but the yield of low-boiling distillate and hydrogenation.

The most notable phenomenon in this comparative study relates to HDS and the use of catalysts F/B\* and LF/B\*. As explained in the experimental section, these catalysts were shaped to a grain rather than an extruded form. Although identical otherwise, the grain catalysts could be estimated to have about 50 times larger external surface area than the extruded catalysts F/B and LF/B, since the average grain size was about 7 times smaller than the average extrudate size. Overall, the grain catalysts performed comparably to the extruded ones, slightly exceeding their performance in hydrogenation and HDN but falling behind in the yield of low boiling and light distillates. However, while comparable in HDN, the grain catalysts outperformed the extruded ones in HDS by a large margin, removing more than twice as much sulphur on the average.

#### Acidity and dispersion

A limited number of acidity measurements were obtained by ammonia adsorption and are shown together with the BET surface areas in Table 4. Both fluoride and lithium impregnation lowered the internal surface area. This was most apparent in case of FF/BL where large amount of fluoride was impregnated causing a loss of about 40 % of the surface area available in B, a negative phenomenon previously attributed to successive impregnation and calcining steps (6). Thus the ammonia adsorption data related to the catalyst weight may be less appropriate than those related to the BET surface area assuming that ammonia could reach into pores accessible to nitrogen. Comparison of these data indicates that fluoride generally increased the surface acidity whereas lithium decreased it but in a more complicated way:

Higher acidity per surface area: FF/BL > LF/B > F/B > B > BL  
Higher acidity per weight: B > LF/B > F/B > FF/BL > BL

Since in the case of BL the dry mixing prevented the chemical interaction possible upon impregnation (LF/B), the surface of  $\text{LiCO}_3$  may have remained exposed, i.e. not covered by metals upon impregnation. Although the same problem likely occurred in FF/BL, the impregnation with large amount of fluoride at the end increased the surface acidity. The interesting finding is that lithium impregnation caused an increase in acidity of LF/B over that of F/B. Although only marginal, this increase happened to be independent of the reference units and thus somewhat more consistent. Since alumina surface doping by lithium impregnation was measured by Vordonis *et al* (7) to decrease the surface acidity, one must consider indirect phenomena leading to an opposite effect in the present catalysts.

One of such indirect phenomena is the influence on dispersion of metals. Previous work by Boorman *et al* (2) and Papadopoulou *et al* (8) pointed out dispersion effects in connection with fluoride doping. It is possible that lithium in LF/B contributed to changes in metal dispersion within F/B accompanied by the increase in acidity.

Subsequent investigations of the doping by fluoride impregnation led to a hypothesis that fluoride enhances cracking but does not lower the hydrogenation capability of molybdenum (4). Results of the present study support such a hypothesis based on the ranking in relative density,

HDN and H/C ratio. As noted earlier, the cracking function seemed to depend on the molecular size, since the ranking in the yield of low-boiling distillates and pitch conversion differed significantly. The role of lithium in lithium-fluoride doping by impregnation is consistent with the acidity tests, slightly emphasizing the hydrogenation rather than cracking functions. The presence of lithium in the mixed support creates sites for cracking of small molecules because of lack of metal dispersion rather than acidity. Here the higher abundance of cracking sites accounts for a lower abundance of hydrogenation sites.

### Diffusion and deactivation

For any reaction, an increase in conversion with decreasing catalyst particle size is often attributed to diffusion. However, two features affecting conversions should be considered in this case - the external surface area and the internal diffusion path. The small particles (grains) of F/B\* and LF/B\* and the large particles (extrudates) of F/B and LF/B have about an equal internal porosity, but the grains differ from the extrudates in the external size. The grain external surface area was estimated to be 50 times larger than the extrudate external surface area. Those molecules with a small chance of accessing the particle interior thus have more opportunity to undergo reaction at the grain external surface than at the extrudate external surface.

It is well known that the rate of diffusion of large molecules of bitumenous oils affects the rate of hydrocracking (9). The grain size was estimated to be about seven times smaller than the extrudate size. The effect of diffusion is such that the concentration of reactants will be greater inside the small grains than inside the extrudates, because the length of the diffusion path to the interior is shorter. In theory (10), the concentration gradient of reactants within the particles can be calculated from the particle size and the ratio of the rate constant and effective diffusivity of the reactants. Orders of magnitudes for these quantities can be estimated (11, 12), and the concentrations at any depth from the external surface can then be shown to be significantly higher within the grains than within the extrudates for some reactions. Such reactions would proceed faster within the grains.

Some phenomena observed in this study can be explained utilizing the two features just discussed. Fig. 1 shows sulphur conversion (HDS) as a function of T.O.S. whereas Fig. 2 shows nitrogen conversion (HDN) as a function of T.O.S., both comparing the performance of catalysts LF/B and LF/B\*. The same graphs could be shown for F/B and F/B\* indicating the same trends. The most obvious observation by comparing Fig. 1 and 2 is that the grains perform much better HDS than extrudates whereas they perform only similar HDN. Another observation, a less obvious one, is that HDN declines with time faster in grains than in extrudates which is accentuated by crossing of the lines in Fig. 2. HDS lines in Fig. 1 do not exhibit such deviations in deactivation trends. Since both HDS and HDN are predominantly catalytic reactions, the differences in catalyst geometry must be the reason for the performance differences observed.

The following explanations can be offered. Surface reactions proceed faster in case of HDS than in case of HDN and thus the diffusional limitations have more influence on HDS. Since the diffusional limitations within extrudates exceed those within grains, the HDS slows down relatively more than HDN when using extrudates. The external surface is unlikely to make a major contribution in either case of HDS or HDN, since the HDN reactions were comparable in the initial stage when the available grain external surface area was about 50 times larger. This in turn would suggest that the very large asphaltenic molecules which do not access the internal surface have probably not reacted significantly. However, the internal surface area within grains (being similar in magnitude to that within extrudates) is more available to large molecules than the internal surface within extrudates because of easier diffusion. Some of these

molecules, especially nitrogenates, are known to deactivate the surface sites by carbonaceous deposits. This would explain the fast HDN deactivation within grains.

The difference between HDS and HDN in deactivation patterns suggests that different sites are used for HDN than for HDS, otherwise the patterns would be similar. The nitrogen removal from an aromatic ring typically requires hydrogenation of the ring as the first step (13, 14). If the hydrogenation sites become poisoned by coke deposits faster than the HDS sites, differences in HDS and HDN deactivation patterns may occur.

## SUMMARY AND CONCLUSIONS

Lithium and fluoride additions to a NiMo/Al<sub>2</sub>O<sub>3</sub> catalyst were evaluated by characterizations and comparative testing with a bitumenous oil. Additional evaluations were done using different external particulate forms. Lithium was either impregnated from an aqueous solution or added in form of an insoluble LiCO<sub>3</sub> powder to the alumina support. In general, fluoride additions were found to cause improvements whereas lithium impediments to hydroprocessing performance. Differences in the particulate size had a very pronounced effect on hydrodesulphurization but not on other aspects of hydroprocessing. The following conclusions and suggestions can be drawn:

- Doping by fluoride impregnation increases both surface acidity and metal dispersion which provide increased hydrocracking activity.
- Adding lithium as support or doping catalysts with lithium impregnation causes a decrease in surface acidity and probably a loss of metal dispersion.
- Doping with both lithium and fluoride impregnations shows a minor but different role for lithium.
- Reducing the diffusional limitations may selectively enhance sulphur removal and impede nitrogen removal.

## REFERENCES

1. Kelly, J.F. and Ternan, M. "Hydrocracking Athabasca bitumen with alkali metal promoted CoO-MoO<sub>3</sub>-Al<sub>2</sub>O<sub>3</sub> catalysts", Can. J. Chem. Eng. 57, 726-733 (1979).
2. Boorman, P.M., Kriz, J.F., Brown, J.R. and Ternan, M., "Hydrocracking bitumen derived from oil sands with sulphided MoO<sub>3</sub>-CoO catalysts having supports of varying composition". Proc. 8th Intl. Congress Catalysis, DEHEMA, Frankfurt am Main, pp. II-281-91 (1984).
3. Boorman, P.M., Kydd, R.A., Sarbak, Z. and Somogyvari, A. "Surface Acidity and Cumene Conversion. I. A study of gamma-alumina containing fluoride, cobalt and molybdenum additives", J. Catal. 96, 115-121 (1985).
4. Boorman, P.M., Kydd, R.A., Sarbak, Z. and Somogyvari, A. "Surface Acidity and Cumene Conversion. II. A study of gamma-alumina containing fluoride, cobalt and molybdenum additives: The effect of reduction", J. Catal. 100, 287-92 (1986).
5. Boorman, P.M., Kydd, R.A., Sarbak, Z. and Somogyvari, A. "Surface Acidity and Cumene Conversion. III. A study of gamma-alumina containing fluoride, cobalt and molybdenum additives: The effect of sulfidation", J. Catal. 106, 544-548 (1987).

6. Lewis, J.M., Kydd, R.A. and Boorman, P.M. "A study of fluorinated Ni-Mo/Al<sub>2</sub>O<sub>3</sub> catalysts in cumene conversion and thiophene HDS reactions", J. Catal. 120, 413-420 (1989).
7. Vordonis, L., Koutsoukos, P.G. and Lycourghiotis, A. "Development of carriers with controlled concentration of charged surface groups in aqueous solutions. II. Modification of gamma-Al<sub>2</sub>O<sub>3</sub> with various amounts of lithium and fluoride ions", J. Catal. 101, 186-94 (1986).
8. Papadopoulou, Ch., Lycourghiotis, A., Grange, P. and Delmon, B. "Fluorinated hydrotreatment catalysts. Characterization and hydrodesulfurization activity of fluorine-nickel-molybdenum / gamma-alumina catalysts", Appl. Catal. 38, 255-271 (1988).
9. Green, D.C. and Broderick, D.H. "Residuum hydroprocessing in the 80's", Chem. Eng. Progr. 77, 33-39 (1981).
10. Satterfield, C.N. "Mass transfer in heterogeneous catalysis", MIT Press, Cambridge Mass., 1970.
11. Altajam, M.A. and Ternan, M. "Hydrocracking Athabasca bitumen using Co-Mo catalysts supported on wide pore carbon extrudates", Fuel 68, 955-960 (1989)
12. Sane, R.C., Webster, I.A. and Tsotsis, T.T. "A study of asphaltene diffusion through unimodal porous membranes", (J.W. Ward ed.) Catalysis 1987, Elsevier, Amsterdam, 1988.
13. Glola, F. and Lee, V. "Effect of hydrogen pressure on catalytic hydrodenitrogenation of quinoline", Ind. Eng. Chem. Proc. Des. Dev. 25, 918-925 (1986).
14. Ho, T.C. "Hydrodenitrogenation catalysis", Catal. Rev. Sci. Eng. 30, 117-160 (1988).



Table 1 - Athabasca bitumen feedstock properties

Relative density, kg/m <sup>3</sup> (15/15°C)	1.009	Major components, wt %:	
Pitch (525°C+), wt %	51.5	Carbon	83.4
Conradson carbon residue, wt %	13.3	Hydrogen	10.5
Pentane insolubles, wt %	16	Sulphur	4.5
Toluene insolubles, wt %	0.7	Oxygen	1.0
Ash (700°C), wt %	0.5	Nitrogen	0.4
		Metals, ppm:	
		Iron	358
		Vanadium	213
		Nickel	67

Table 2 - Catalyst specifications

Catalyst ID	Type	Li:F: Ni:Mo:Al atomic ratios (Ni:Mo:Al = 1:2:30 in each case)
B	NiMo/Al <sub>2</sub> O <sub>3</sub>	0:0:1:2:30
F/B, F/B*	F-NiMo/Al <sub>2</sub> O <sub>3</sub>	0:3: ...
LL/B	Li-NiMo/Al <sub>2</sub> O <sub>3</sub>	3:0: ...
LF/B, LF/B*	Li-F-NiMo/Al <sub>2</sub> O <sub>3</sub>	1:3: ...
BL	NiMo/Al <sub>2</sub> O <sub>3</sub> -Li <sub>2</sub> CO <sub>3</sub>	3:0: ...
F/BL	F-NiMo/Al <sub>2</sub> O <sub>3</sub> -Li <sub>2</sub> CO <sub>3</sub>	3:3: ...
FF/BL	F-NiMo/Al <sub>2</sub> O <sub>3</sub> -Li <sub>2</sub> CO <sub>3</sub>	3:6: ...

Table 3 - Liquid product analyses

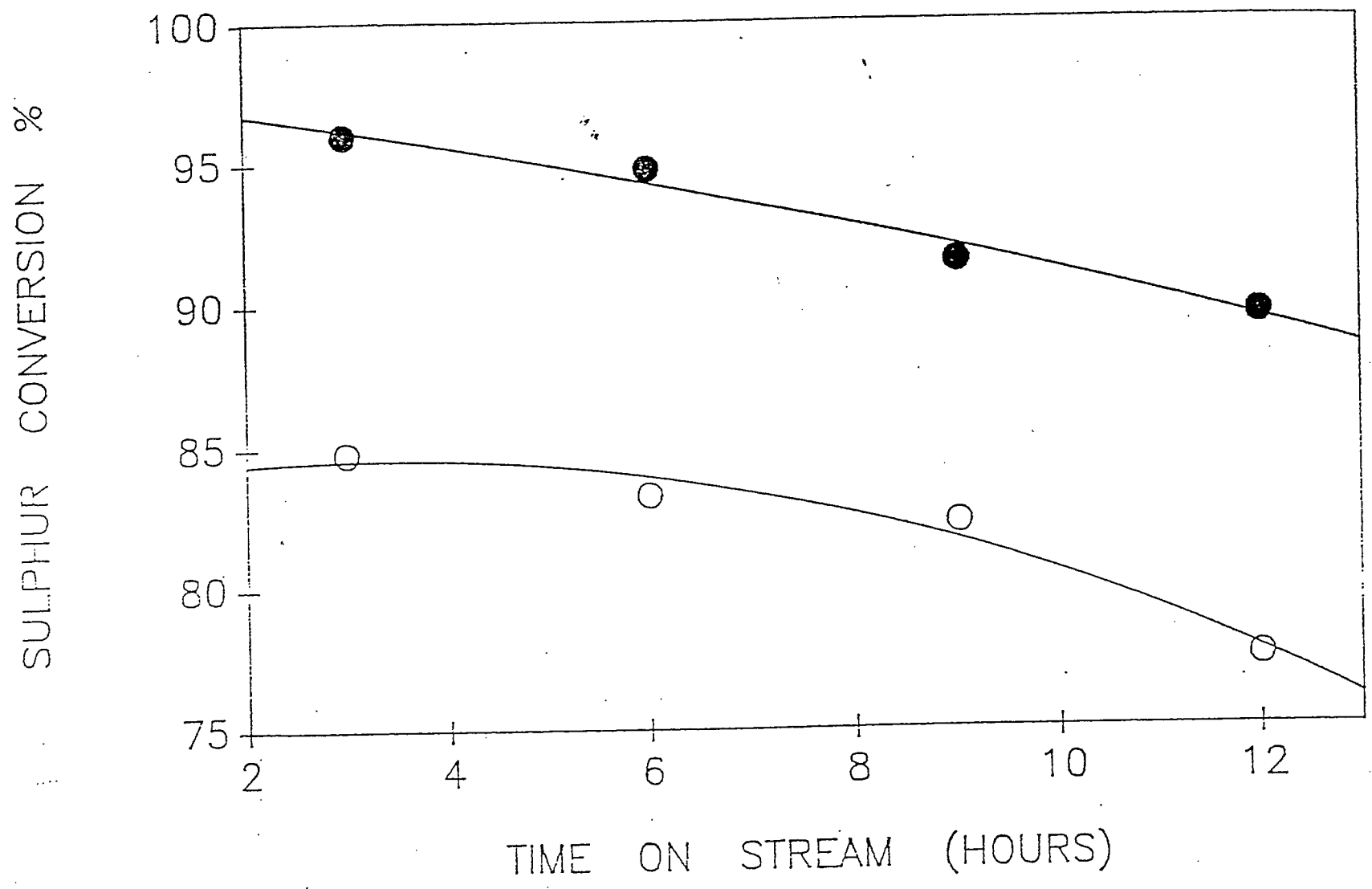
Catalyst ID	T.O.S. h	Product density g/mL	S wt %	N wt %	H wt %	C wt %	525°C+ wt %	10 % off °C	50 % off °C
B	3	0.9204	0.81	0.246	11.7	86.8	0	230	363
	6	0.9215	0.87	0.256	11.8	86.7	3	235	367
	9	0.9244	0.99	0.266	11.7	86.6	0	238	362
	12	0.9254	1.00	0.270	11.8	86.5	2	237	366
F/B	3	0.9135	0.78	0.194	11.9	86.4	4	235	360
	6	0.9155	0.84	0.206	11.9	86.6	6	236	361
	9	0.9177	0.92	0.216	11.8	86.4	6	235	360
	12	0.9204	1.18	0.216	11.8	86.4	5	236	361
F/B*	3	0.9117	0.28	0.152	12.1	87.1	1	256	374
	6	0.9184	0.27	0.205	12.1	86.9	3	258	378
	9	0.9205	0.35	0.200	12.0	87.1	4	259	380
	12	0.9235	0.42	0.235	11.8	87.2	6	261	382

LL/B	3	0.9202	0.92	0.270	11.8	86.8	1	212	362
	6	0.9242	1.01	0.294	11.7	86.7	4	225	370
	9	0.9282	1.17	0.296	11.7	86.7	5	233	365
	12	0.9293	1.15	0.300	11.7	86.7	5	237	371
LF/B	3	0.9135	0.75	0.200	11.9	86.5	3	238	359
	6	0.9164	0.83	0.200	12.0	86.4	4	239	362
	9	0.9184	0.88	0.228	11.8	86.4	4	238	360
	12	0.9204	1.11	0.228	11.9	86.4	4	239	362
LF/B*	3	0.9145	0.21	0.165	12.0	87.3	6	255	381
	6	0.9194	0.27	0.195	12.1	87.1	6	257	380
	9	0.9234	0.41	0.219	11.9	87.0	7	263	385
	12	0.9253	0.52	0.264	11.9	86.9	8	261	386
LLF/B	3	0.9166	0.74	0.196	12.0	86.5	12	247	382
	6	0.9208	0.85	0.206	12.0	86.6	10	248	378
	9	0.9238	0.91	0.222	11.8	86.6	6	244	369
	12	0.9252	1.02	0.216	11.8	86.6	6	246	372
BL	3	0.9261	0.98	0.290	11.8	86.8	7	244	373
	6	0.9271	1.03	0.157	11.7	86.9	6	243	371
	9	0.9300	1.02	0.320	11.7	86.6	10	325	438
	12	0.9311	1.07	0.323	11.7	86.7	9	238	430
F/BL	3	0.9206	0.85	0.250	11.9	86.7	7	234	421
	6	0.9221	0.90	0.258	11.9	86.9	8	239	425
	9	0.9255	1.05	0.278	11.8	86.4	8	224	418
	12	0.9265	1.06	0.283	11.8	86.6	7	226	419
FF/BL	3	0.9158	0.78	0.255	11.9	86.7	6	233	419
	6	0.9208	0.87	0.228	11.9	86.8	7	232	422
	9	0.9258	0.95	0.256	11.7	86.6	8	248	427
	12	0.9268	1.03	0.260	11.7	86.7	7	249	429
F/B*	3	0.9117	0.20	0.134	12.1	87.3	1	251	375
	6	0.9184	0.26	0.164	12.1	87.2	3	252	379
	9	0.9205	0.34	0.181	12.0	87.4	4	255	380
	12	0.9235	0.40	0.216	11.9	87.1	6	259	385

Table 4 - Catalyst surface characterizations

Catalyst	BET surface area, m <sup>2</sup> /g	umol NH <sub>3</sub> /g	molecules NH <sub>3</sub> /nm <sup>2</sup>
B	299	305	0.612
F/B	243	284	0.705
LF/B	248	301	0.730
BL	232	184	0.478
FF/BL	177	253	0.860

Li-T on Ni-Mo/Al<sub>2</sub>O<sub>3</sub> powder



2

